

HIGH-SENSITIVITY DETECTION OF XENON ISOTOPES VIA BETA-GAMMA COINCIDENCE COUNTING

Ted W. Bowyer, Justin I. McIntyre, Paul L. Reeder
Pacific Northwest National Laboratory

Sponsored by U. S. Department of Energy
Office of Nonproliferation and National Security
Office of Research and Development
Contract No. DE-AC06-76RLO 1830

ABSTRACT

Measurement of xenon fission product isotopes is a key element in the global network being established to monitor the Comprehensive Nuclear-Test-Ban Treaty. Pacific Northwest National Laboratory has developed an automated system for separating Xe from air which includes a beta-gamma counting system for ^{131m}Xe , ^{133m}Xe , ^{133}Xe , and ^{135}Xe . Betas and conversion electrons are detected in a plastic scintillation cell containing the Xe sample. The counting geometry is nearly 100% for beta and conversion electrons. The resolution in the pulse height spectrum from the plastic scintillator is sufficient to observe distinct peaks for specific conversion electrons. Gamma and X-rays are detected in a NaI(Tl) scintillation detector which surrounds the plastic scintillator sample cell. Two-dimensional pulse height spectra of gamma energy versus beta energy are obtained. Each of the four xenon isotopes has a distinctive signature in the two-dimensional energy array. The details of the counting system, examples of two-dimensional beta-gamma data, and operational experience with this counting system will be described.

Key Words: Xenon Fission Products, Beta-Gamma Coincidence Counting, CTBT Monitoring

OBJECTIVE

1. Relevance to CTBT

Clandestine underground nuclear tests are likely to vent Xe fission product gases into the atmosphere. As called for by the Comprehensive Nuclear-Test-Ban Treaty (CTBT), the International Monitoring System includes xenon monitoring systems to detect any such releases [1]. These systems must be extremely sensitive because of the dilution of the Xe gases during atmospheric transport to the monitoring station. Present requirements specify that the four isotopes ^{131m}Xe , ^{133m}Xe , ^{133}Xe , and ^{135}Xe be measured, that ^{133}Xe be measured with a sensitivity of $<1 \text{ mBq/m}^3$, and that the measurement system be suitable for automatic operation in remote locations.

2. Significance of each isotope

The four isotopes of Xe to be measured for CTBT have varying degrees of usefulness as indicators of a nuclear weapons explosion [2]. However, any or all of them may be present in routine air samples so it is important to quantify them so that anomalous concentrations can be evaluated.

The nuclide ^{131m}Xe ($t_{1/2} = 11.93 \text{ d}$) is produced in low yield from nuclear explosions - several orders of magnitude below that of ^{133}Xe and ^{135}Xe . However, it is formed as a by-product of ^{133}Xe production for use in medical procedures. It can be present in airborne samples as a result of accidental releases from medical facilities, during operation of nuclear reactors, or from dissolution of spent reactor fuel. Although it is not a major indicator of a nuclear explosion, it is a potential interference in measurements of the other Xe isotopes. It is also used as a convenient source to calibrate the beta-gamma counting system. In those cases where there is a long time delay between a nuclear explosion and collection of the sample, an elevated level of ^{131m}Xe may be the only indicator of a weapons violation because the ^{131m}Xe half-life is longer than the other Xe fission products.

The ^{133m}Xe is present in air samples primarily as the result of a process involving its independent fission yield - most likely, the result of a nuclear explosion. Because ^{133m}Xe is produced in only 2.9% of ^{133}I decays, its cumulative fission yield relative to ^{133}Xe is quite small. Most of the Xe released during reactor operations or fuel reprocessing results from decay of the precursor I isotopes (cumulative yield) which results in low ratios of ^{133m}Xe to ^{133}Xe . Also, the method of thermal neutron capture on stable Xe isotopes used to produce ^{133}Xe for medical purposes yields almost 10 times as much ^{133}Xe as ^{133m}Xe . Thus, a high quantity of ^{133m}Xe as well as a high ratio of ^{133m}Xe to ^{133}Xe in a given air sample is a key indicator of a nuclear weapons test.

The most likely Xe nuclide seen in ambient air samples is ^{133}Xe . This is often observed in locations downwind from nuclear power plants or perhaps from medical facilities. Its 5.25 d half-life and large cumulative fission yield are factors contributing to its detectability. The PNNL Xe monitoring system routinely observed ^{133}Xe in samples of New York City air and occasionally in samples of air taken in central Florida [3]. The yields of ^{133}Xe seen in these locations are highly variable depending on weather conditions. At our laboratory in eastern Washington state, we rarely observe ^{133}Xe in ambient air as we are upwind of the only reactor in our area. At island locations in the southern hemisphere, levels of ^{133}Xe in ambient air should be negligible. Thus, it will be essential to monitor the baseline levels of ^{133}Xe at each monitoring station. A large increase in ^{133}Xe concentrations above typical fluctuations would be an indication of a possible treaty violation.

Both the independent and the cumulative fission yields of ^{135}Xe are quite large. However, the short half-life for ^{135}Xe ($t_{1/2} = 9.14 \text{ h}$) imposes restrictions on the distance over which this nuclide can travel between its source and the Xe sampling station. In the absence of any near-by sources such as nuclear power reactors, the presence of ^{135}Xe is another clear indication of a nuclear weapons test.

3. Isotopic signatures

The four Xe isotopes of interest for CTBT have distinctive radioactive decay properties which allow them to be distinguished from each other in a suitably designed detection system. These decay properties are given in Table 1 along with their radioactive half-lives and fission yields. The independent fission yields are more likely to be associated with nuclear weapons explosions whereas the cumulative fission yields are more closely associated with reactor operations or spent fuel operations.

Table 1. Half-lives, fission yields, principal radiations and abundances of Xe fission products.^{a,b}

Nuclide	^{131m} Xe	^{133m} Xe	¹³³ Xe	¹³⁵ Xe
<u>Half-life</u>	11.93 d	2.19 d	5.25 d	9.14 h
<u>Fission yield</u>				
Independent (%)	2.41 x 10 ⁻⁷	4.23 x 10 ⁻³	1.46 x 10 ⁻³	1.20 x 10 ⁻¹
Cumulative (%)	4.51 x 10 ⁻²	1.98 x 10 ⁻¹	6.72 x 10 ⁰	6.60 x 10 ⁰
<u>Photon Emission</u>				
Energy (keV)	163.9	233.2	81.0	249.8
Abundance (%)	1.96	10.3	37.0	90.0
<u>X-ray Emission</u>				
(K-shell)				
Energy (keV)	30.	30.	31.	31.
Abundance (%)	54.05	56.3	48.9	5.2
(L-shell)				
Energy (keV)	4.3	4.3	4.5	4.5
Abundance (%)	7.2	6.8	5.2	0.6
<u>Beta Spectrum</u>				
Max. Energy (keV)			346.	905.
Ave. Energy (keV)			99.	300.
Abundance (%)			99.	97.
<u>Conversion. Electrons</u>				
(K-shell)				
Energy (keV)	129.	199.	45.	214.
Abundance (%)	60.7	63.1	54.1	5.7
(L-shell)				
Energy (keV)	159.	229.	75.	245.
Abundance (%)	37.4	26.9	8.4	1.1

^aHalf-lives and decay data are from the Table of Radioactive Isotopes [4].

^bFission yields are for fast fission of ²³⁵U [5].

The nuclide ^{131m}Xe is an isomeric state which decays to the ground state of ¹³¹Xe by a 163.9-keV transition. The 163.9-keV gamma is highly converted and can not be seen in gamma singles counting above the normal backgrounds. However, the coincidence between the 129-keV conversion electrons and the 30-keV X-rays of Xe provides a unique signature in a beta-gamma counting system. With a low-noise NaI(Tl) detector, the 4.3-keV X-rays can be observed in coincidence with the 159-keV conversion electrons.

The nuclide ^{133m}Xe has a similar decay scheme as ^{131m}Xe. Its 233.2-keV gamma is also difficult to see in gamma singles counting, but the 30-keV X-rays in coincidence with its conversion electrons at 199 keV are efficiently detected in a beta-gamma counting system. With a low-noise NaI(Tl) detector, the 4.3-keV X-rays can be observed in coincidence with the 229-keV conversion electrons.

The dominant beta decay branch (99.2%) of ¹³³Xe populates the first excited state of ¹³³Cs which deexcites by emission of an 81-keV gamma or by internal conversion producing conversion electrons and Cs X-rays. The coincidence between the beta particles and the 81-keV gamma is a distinctive signature for ¹³³Xe. However, the 81-keV gamma appears in only 37% of the ¹³³Xe decays due to internal conversion. The conversion electrons are counted along with the preceding betas by the beta detector. A second signature for ¹³³Xe is the coincidence between the betas plus conversion electrons with the 31-keV X-rays of the Cs daughter.

The distinctive signature for ¹³⁵Xe is its 249.8-keV gamma in coincidence with the preceding beta particle.

To make use of these individual signatures, it is necessary to measure the energy spectrum of the gamma and X-rays in coincidence with the energy spectrum of the betas and conversion electrons as described below.

II. RESEARCH ACCOMPLISHED

In support of the CTBT monitoring program, the Pacific Northwest National Laboratory (PNNL) has developed an automated system for separating Xe from air and counting the Xe fission-product nuclides [3][6]. The system is called ARSA which stands for Automated Radioxenon Sampler-Analyzer. The PNNL system extracts the few cm^3 of Xe contained in 48 m^3 of air by use of cryogenic techniques and selective adsorption on charcoal as described elsewhere in this symposium. The Xe samples are counted with a beta-gamma coincidence system which has high sensitivity for $^{131\text{m}}\text{Xe}$, $^{133\text{m}}\text{Xe}$, ^{133}Xe , and ^{135}Xe [7] [8] [9]. Samples are contained in hollow plastic scintillation cells surrounded by two NaI(Tl) detectors. Pulse height spectra for beta particles and/or conversion electrons detected by the plastic scintillator are recorded in coincidence with the pulse height spectra of gammas and X-rays detected by the NaI(Tl) scintillator. These pulse height data are stored in a two-dimensional array of gamma (photon) energy versus beta (electron) energy as described below. Each of the four Xe isotopes of interest occupies a distinctive location within the two-dimensional array. Background radiations are largely eliminated by the coincidence requirement between the plastic scintillator and the NaI(Tl) scintillator. The use of beta-gamma coincidence counting provides identification of each isotope under very low-background conditions and thus gives the required high sensitivity for detection of Xe fission products.

1. Description of detector

a. Hardware

The beta-gamma counting system contains two rectangular NaI(Tl) detectors sandwiched together in a single aluminum can with a light barrier between them. Each crystal is viewed by two 7.62-cm diam. photomultiplier tubes (PMTs). The outputs of the two PMTs are gain matched and summed to provide uniform pulse height resolution over the long dimension of the crystal. The arrangement of crystals and PMTs is illustrated in Fig. 1.

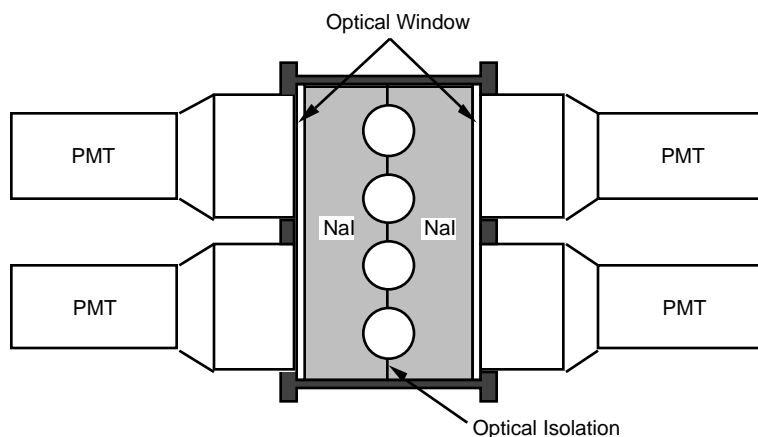


Fig. 1. NaI(Tl) scintillation detectors for Xe monitoring system. Plastic scintillator sample cells occupy the four holes in the NaI(Tl) detectors.

Four holes with diameters of 3.175 cm are machined in the plane defined by the light barrier between the two crystals. These holes contain the plastic scintillation cells that contain the Xe samples and detect the beta particles. This detector package allows the simultaneous counting of four samples. The scintillation cells are cylinders with outside dimensions of 5.08-cm length by 1.51-cm diam. having 0.12-cm thick walls and 0.10-cm thick end plugs giving an internal volume of 6.18 cm^3 . The arrangement of sample cell and phototubes is illustrated in Fig. 2. A single gas transfer line is used to insert and remove the Xe sample. The figure does not show the additional transfer tubes which allow an external calibration source to be moved to the midpoint of the cell.

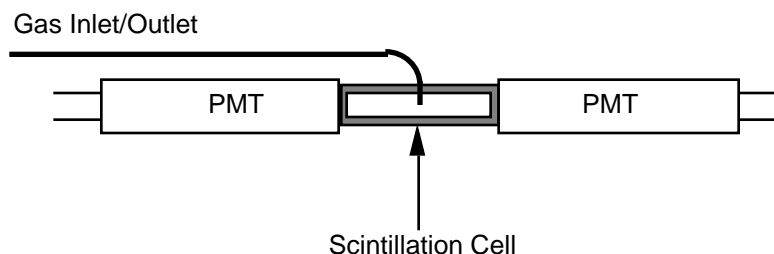


Fig. 2. Schematic representation of plastic scintillation sample cell and photomultiplier tubes.

The plastic scintillator walls are thick enough to completely stop all betas from ^{133}Xe . The ends of the scintillation cells are viewed by 1.90-cm diam. Thorn 9078SA PMTs. The two PMTs are operated in coincidence so that PMT dark current pulses are rejected.

b. Electronics

The electronics described in our previous publications were designed to provide beta-gated gamma spectra only [3][7][8][9]. These electronics have now been modified to provide both the gamma spectra and the beta spectra in a two-dimensional histogram array. The pulse height spectra from the two halves of the NaI(Tl) detector are gain matched and multiplexed together to provide a single gamma pulse height spectrum. However, logic pulses are generated for events in each half of the NaI(Tl) detector. Valid events are those for which only one of the two halves has an event. This requirement allows the rejection of Compton scattering events in which a gamma scatters from one half of the detector into the other half and also allows the rejection of cosmic ray events which traverse both detectors.

The pulses from the two PMTs at each end of a single beta cell are summed together before being shaped for pulse height analysis. Gain matching of these two PMTs must be performed to optimize the pulse height resolution for the beta spectrum. Logic pulses are created for each of the four xenon sample cells. The beta pulses are multiplexed to a single analog-to-digital converter (ADC). However, the beta logic pulses are used to route the pulse height data to four separate gamma versus beta two-dimensional arrays in the computer. Multiplexing of the beta and gamma signals to a single gamma ADC and a single beta ADC simplifies the electronics and is possible because of the low count rates in all the detectors. Typical gamma singles count rates are about 50 to 100 cps when the detector is within the 5.08-cm thick lead shield whereas the beta count rates in a single cell are about 1 cps.

All of the electronics used for the radiation detection are commercial NIM modules except for the interface module which transfers the two gamma logic pulses, the four beta logic signals, the gamma pulse height address, and the beta pulse height address to the computer. Currently, the data acquisition computer is the same QNX-based computer which controls the xenon collection and purification process.

c. Calibrations

For relatively simple decay schemes, the efficiency of a particular detector can be determined by coincidence counting without knowing the absolute disintegration rate of the source. The counting rate in the beta detector (R) is given by the source strength (R_o) times the beta detection efficiency (ϵ) times the abundance of the beta (A). The beta-gamma coincidence rate (R_c) is given by the source strength times the beta efficiency times the beta abundance times the gamma efficiency (ϵ_g) times the gamma abundance (A_g). Thus the beta efficiency is determined from the following expression.

$$\frac{R_c}{R} = \frac{R_o \epsilon_g A_g}{R_o \epsilon A} = \epsilon_g \frac{A_g}{A} \quad \text{Eq. (1)}$$

Thus, the beta efficiency is determined simply by measuring the beta-gamma coincidence rate and the gamma singles rate. The beta abundance is known from the decay scheme.

Calibration of the beta efficiency for ^{133}Xe is best done with a spike sample of pure ^{133}Xe available from commercial suppliers. The number of counts in the beta-gated gamma peak at 81 keV divided by the

number of counts in the ungated 81-keV gamma peak is the beta efficiency associated with that gamma peak. Note that the beta abundance as given in Table 1 is essentially 100%. The same procedure gives the beta counting efficiency for the betas and conversion electrons in coincidence with the 31-keV X-rays. The counting efficiency for the combined betas plus conversion electrons is greater than the counting efficiency for the betas alone because the extra pulse height contributed by the conversion electrons puts more of the events above the low-level discriminator threshold. Experimentally, we measure a counting efficiency for the betas associated with the 81-keV gamma from ^{133}Xe of about 75% whereas the betas and conversion electrons associated with the 31-keV X-rays have an efficiency of 97%. Although we do not have experimental efficiencies for the conversion electrons associated with $^{131\text{m}}\text{Xe}$ and $^{133\text{m}}\text{Xe}$, the energies of the conversion electrons from these two isotopes are greater than most of the betas from ^{133}Xe so we expect the conversion electron counting efficiencies to be greater than 95%. For ^{135}Xe , the beta spectrum extends to a maximum energy about 3x the maximum energy of the ^{133}Xe beta spectrum so we expect beta efficiencies greater than 90% for ^{135}Xe .

The calibration of the gamma efficiencies for ^{133}Xe could be done in a similar fashion. However, an extra correction factor is required to account for the fact that not all beta events have the same counting efficiency and the gamma abundances are not unity. This correction factor is dependent on knowing the beta efficiencies for each of the beta processes and the gamma abundance factor. For ^{133}Xe , the efficiency for the 81-keV gamma is the number of counts in the beta-gated 81-keV gamma peak divided by the number of counts in the ungated beta spectrum times the correction factor. The experimental value for this efficiency is 84% for the sum of the two NaI(Tl) detectors. This efficiency value includes the small iodine escape peak at 52 keV. Without the escape peak, the efficiency is 80%. The efficiency for the 31-keV X-ray peak is the number of counts in the beta-gated 31-keV peak divided by the number of counts in the ungated beta spectrum times a different correction factor. The experimental efficiency for the 31-keV X-ray is 67%. It is not surprising that the 31-keV X-rays are less efficient than the 81-keV gamma because the X-rays have a higher absorption probability while traversing the plastic scintillator cell, the sample cell holder, and the hermetic can surrounding the NaI(Tl) detector. It is expected that the gamma detection efficiency will first increase as a function of gamma energy and then decrease at energies above 100 keV. Thus the gamma detection efficiency for the 249.8-keV gamma from ^{135}Xe should be about 30% less than the efficiency for the 81-keV gamma. As an alternative procedure, we are currently calibrating the gamma efficiencies using a mixed isotopic source with calibrated intensities.

2. Rn interference

A major requirement of the xenon collection and purification system is to provide a xenon sample free of radon gas. The ^{238}U found naturally throughout the world decays through a chain of alpha and beta decays to ^{222}Rn which has a 3.8 d half-life. The amount of ^{222}Rn present in ambient air is variable depending on location and weather conditions but normally is in far greater concentration than the desired xenon isotopes. If any ^{222}Rn is transferred into the xenon sample cell, it produces two beta-decaying daughter isotopes, ^{214}Pb and ^{214}Bi , which are readily observed by the beta-gamma counting system and interfere with measurements of the xenon radioactivities.

An example of a two-dimensional (2D) histogram array of gamma pulse height versus beta pulse height is shown in the left hand plot of Fig. 3 for a sample containing ^{222}Rn gas and no radioactive Xe gas. The energy scale of the gamma axis has been adjusted to include the 609.3-keV gamma ray following beta decay of ^{214}Bi . The gain on the beta axis has also been adjusted to see the maximum pulse heights produced by the betas from ^{214}Pb and ^{214}Bi .

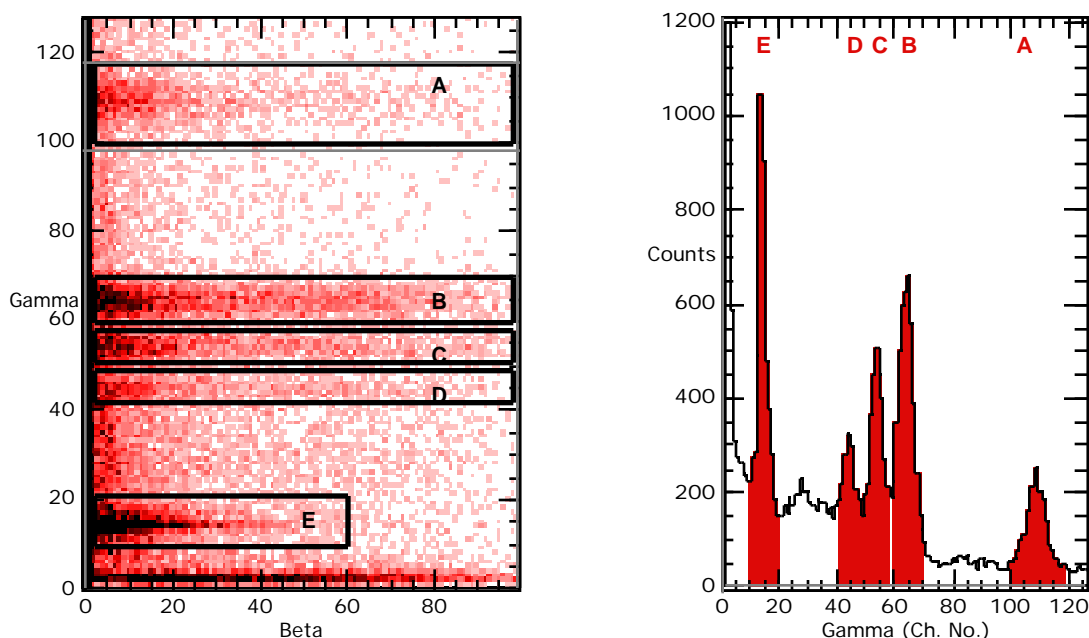


Fig. 3. Left hand plot is two-dimensional array of gamma pulse height versus beta pulse height for Rn sample. Axes are labeled with channel numbers. Gray scale indicates relative number of counts. Right hand plot is gamma spectrum obtained from the same data by integration along the beta axis.

These pulse heights are greater than the pulse heights observed for the xenon isotopes. The right hand plot of Fig. 3 shows the one-dimensional gamma spectrum obtained by integrating the counts along the beta axis between beta channels 2 through 99. The regions of interest labeled A - E in the 2-D array of Fig. 3 correspond to the following radiations.

- A. 609.3-keV gamma ray following beta emission from ^{214}Bi .
- B. 351.9-keV gamma ray following beta emission from ^{214}Pb .
- C. 295.1-keV gamma ray following beta emission from ^{214}Pb .
- D. 241.9-keV gamma ray following beta emission from ^{214}Pb
- E. X-rays with energies between 75- and 90-keV from ^{214}Pb plus a small contribution (10%) of X-rays between 77- and 92-keV from ^{214}Bi .

The shaded areas and labels in the right hand plot of Fig. 3 correspond to the regions of interest defined in the left hand plot.

The 241.9-keV gamma from ^{214}Pb interferes with observation of the 249.8-keV gamma from ^{135}Xe while the X-rays from Pb and Bi decays interfere with observation of the 81-keV gamma from ^{133}Xe . Fortunately the areas of each peak in these spectra are constant relative to each other so knowing the area under the 351.9-keV peak, for example, in an actual xenon spectrum allows one to calculate the counts due to ^{214}Pb and ^{214}Bi corresponding to their X-ray peak and the 241.9-keV peak. These calculated areas can then be used to correct the observed areas in the xenon spectra. Because the beta pulse height spectra for the desired xenon isotopes have lower amplitudes than the beta pulse height spectra for the interferences, we can choose regions of interest in the 2-D arrays which minimize the contribution from the interferences.

3. 2-D spectrum of Xe from U fission

An experiment to measure Xe gases from fission of ^{235}U was conducted. A thin sample of ^{235}U was irradiated at a reactor and allowed to cool in a sealed container for about 1 day. Then a syringe was inserted into the gas space surrounding the sample and a small volume of gas was removed. This gas was then injected without further purification into a xenon sample cell and counted at 4 hour intervals over several days. A typical 2D histogram array is shown in Fig. 4 along with the same data integrated to give the gamma spectrum gated by betas of all energies.

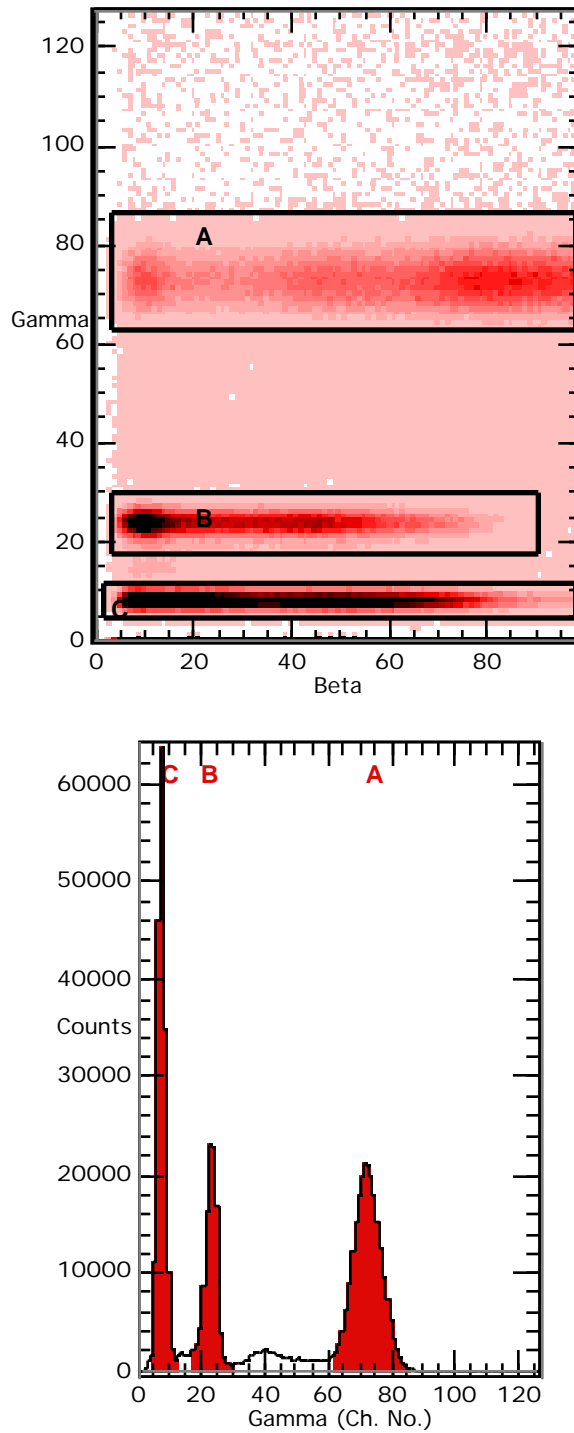


Fig. 4. Left hand plot is two-dimensional array of gamma pulse height versus beta pulse height for Xe fission gas sample. Axes are labeled with channel numbers. Gray scale indicates relative number of counts. Right hand plot is gamma spectrum obtained from the same data by integration along the beta axis.

a. Identification of ROI's

The boxes labeled A, B, and C in the 2D plot in Fig. 4 correspond to regions of interest for particular Xe isotopes. Region A is centered on the gamma peak at 250 keV and the beta spectrum corresponding to the 905-keV betas from ^{135}Xe . The energy scale for this particular experiment did not allow observation of the highest energy beta pulses for this isotope. Region B is centered on the 81-keV gamma and 346-keV betas from ^{133}Xe . Region C is centered on the 31-keV X-rays and betas plus conversion electrons also from ^{133}Xe . Note that the betas and conversion electrons from ^{133}Xe are observed simultaneously in the plastic scintillator so that the energy of the conversion electrons shifts the beta spectrum to somewhat greater pulse heights than for the beta spectrum observed with the 81-keV gamma.

The shaded areas in the gamma spectrum shown in the right hand plot of Fig. 4 indicate the corresponding regions of interest. The small peak at about channel 40 on the gamma axis is the result of the fortuitous overlap of the Compton edge and Compton backscatter peaks for an incident gamma energy of 250 keV. The conclusion that this peak is associated with ^{135}Xe is confirmed by the half-life analysis described below.

Because of the time delay before collecting the xenon gas sample, much of the ^{133}I had decayed to ^{133}Xe thus increasing the abundance of the ^{133}Xe at the expense of $^{133\text{m}}\text{Xe}$. As a consequence, the conversion electron peak at 200 keV in coincidence with the 30-keV X-rays for $^{133\text{m}}\text{Xe}$ was somewhat obscured. Likewise, the signature for $^{131\text{m}}\text{Xe}$ is not expected for this set of data because of the low independent yield of ^{131}Xe . The long half-life of ^{131}I (8 days) prevents it from contributing to the cumulative yield of $^{131\text{m}}\text{Xe}$ in this experiment.

b. Half-life analysis

Two-dimensional pulse height spectra were obtained for the xenon fission products as a function of time over a period of about 7 days. Various regions of interest like those illustrated in Fig. 4 were integrated to obtain the number of counts as a function of time. These data were analyzed using a least squares fitting program which accounted for growth and decay and branchings for all xenon isotopes. For gamma energies greater than 100 keV, all the regions of interest could be fitted with just two components corresponding to decay of ^{135}Xe and a flat background. Regions of interest restricted to gamma energy of 80 ± 20 keV were fitted using 4 components – decay of ^{133}Xe , growth and decay of ^{133}Xe from decay of $^{133\text{m}}\text{Xe}$, a small contribution from ^{135}Xe , and a flat background. The decay curves corresponding to 30 ± 10 keV-gamma energy were quite complex as $^{133\text{m}}\text{Xe}$, ^{135}Xe , and ^{133}Xe all contribute X-rays in this region. From the initial activities calculated from a fit to the 30 ± 10 -keV region which included all beta energies, we calculated that the xenon fission gas sample at the time of extraction from the ^{235}U target had 13% $^{133\text{m}}\text{Xe}$, 75% ^{133}Xe , and 12% ^{135}Xe (atom %) which is in rough agreement with expectations based on cumulative fission yields. As expected, when the same region of interest was limited to only the highest beta energy (channels 95 - 99 in Fig. 4), the decay curve could be fitted with only a ^{135}Xe component and a flat background component.

Normally, the ARSA system will not perform half-life analysis. Identification of specific isotopes will be based on relative numbers of counts within a specific region of interest associated with individual signatures. However, the 2D spectra and half-life analysis performed in this experiment illustrates that the ARSA counting system does measure all the xenon isotopes of interest for CTBT purposes.

5. Factors affecting performance

The 2D histogram arrays of gamma energy versus coincident beta energy provide a highly selective and sensitive technique for identification and quantification of particular xenon isotopes. However, there are several factors which degrade the performance and which should be avoided whenever possible.

The only radioactive gas which interferes is ^{222}Rn . The signatures from the ^{214}Pb and ^{214}Bi daughters were shown above in Section II.2. If ^{222}Rn is not completely removed by the xenon separation system, the daughter signatures will be observed in the counting data. However, using the regions of interest defined in Fig. 3, the number of counts in region B (352-keV gamma) will be in a fixed ratio to the number of counts in regions D and E. These fixed ratios can be used with the observed number of counts in region B to

provide an accurate correction for the Rn daughters that might interfere with the xenon isotopes whose signatures occur near regions D and E. Because of possible errors in making such corrections, it is desirable to minimize any contamination of the xenon sample with radon.

Another factor affecting performance is the incomplete removal of one xenon sample before inserting a new xenon sample. We have observed that a small fraction (5%) of a xenon sample remains in the sample cell even after prolonged pumping on the cell. Thus, if a low activity xenon sample is counted after a preceding sample with high activity levels, the residual activity can bias the result for the low activity sample. To correct for this effect, we always take a background count before each sample count and use any residual xenon activity in the background count to correct the sample count.

A third factor affecting performance is the variability of the concentrations of xenon radioisotopes in ambient air due to human activities related to medical uses of xenon isotopes or to reactor operations. These variations will be dependent on the location of the sampling station, weather conditions, and the human activities. It will be necessary to establish baseline concentrations of each of the four isotopes at each of the sampling stations and to observe these concentrations over some period of time to establish normal variations in these concentrations. In any case, a high concentration of ^{133m}Xe would be immediate cause for further investigation.

III. CONCLUSIONS AND RECOMMENDATIONS

1. Minimum detectable concentrations

The data shown in Section II.3 for xenon fission gas are for a laboratory test and are not representative of typical counting data for ambient air. Results from ambient air samples taken over several months in New York City have been described in our previous publication [3]. ^{135}Xe was observed only on a few occasions as a result of releases from nearby reactors. Variable concentrations of ^{133}Xe up to 60 mBq/m^3 were observed routinely as a result of reactor releases or medical usage. The counting system used during the New York tests did not involve measurement of the beta spectra so the concentrations of ^{131m}Xe and ^{133m}Xe could not be separated from each other. However, the combined concentration was always weak or not observed.

The results of the New York tests lead to the estimates of minimum detectable concentrations (MDC) shown in Table 2 for the various isotopes[10]. These values are based on 16 hours of counting per sample and stable xenon yields of about 1 cm^3 . The range of MDCs for ^{133}Xe is primarily due to memory effects following intentional spike samples.

Table 2. Minimum detectable concentrations of xenon fission product isotopes based on 2 uncertainties.

Isotope	MDC (mBq/m ³)
$^{131m}\text{Xe} + ^{133m}\text{Xe}$	0.8
^{133}Xe	0.14 to 0.34
^{135}Xe	0.18

More recently, the ARSA system gives about 2 cm^3 of Xe and samples are counted for 24 h instead of 16. Thus the MDCs now are even lower than those given in Table 2. Samples are collected for about 8 h so these results are available three times per day. The current specification for CTBT monitoring for ^{133}Xe is 1 mBq/m^3 so the ARSA system easily meets this requirement. The CTBT specifications are not defined for the other Xe isotopes because they depend critically on the detection system used. The 2D counting data for the ARSA system reported here will enable determination of all four Xe isotopes, but we do not yet have results for the MDCs of ^{131m}Xe and ^{133m}Xe separately.

2. Program status and directions

The ARSA system has been developed over the past few years with several prototype systems of increasing sophistication. The development program is continuing with the goal of reducing the size and power requirements of the system. One of the requirements of the earlier prototypes was to use commercial NIM electronics wherever possible. We are currently designing dedicated counting electronics which will minimize the electronics package. At present, there are two copies of the latest ARSA system. One is in

operation at PNNL and the other is at DME Corp. in Orlando, FL. DME Corp. has been given the task of producing a commercial version of the ARSA system based on the current PNNL prototype.

a. Monte Carlo modeling

Recently, we have begun a program of Monte Carlo calculations to model the response of the plastic scintillator and NaI(Tl) detectors to various radiations. Because of the unusual shape of the xenon sample cell, its response to internal xenon beta and conversion electrons is of great interest. In addition, the response to the external calibration sources is needed. Previously, we have used an external source containing equal amounts of ^{154}Eu and ^{155}Eu to establish amplifier gains for the beta detectors and to monitor the detector performance over time. We now plan to use an external source containing ^{154}Eu and ^{207}Bi . The ^{207}Bi calibration source has conversion electrons at 482 keV and 976 keV which greatly simplify adjusting the beta amplifier gains. The 482-keV conversion electrons lose much of their energy in the first wall of the sample cell and the rest of their energy in the second wall. The conversion electrons at 976 keV have enough energy to pass completely through both walls of the sample cell. However, electrons can undergo large angle scattering in the plastic and thus the 976 keV electrons could deposit all of their energy some fraction of the time. This complicated response will be modeled and compared to the response observed experimentally.

b. Phase I, II, III testing

The CTBT Preparatory Commission has requested a test of xenon analysis systems to assess the state-of-the-art for current technology. Currently there are four countries (France, Russia, Sweden, and USA) which have systems designed to meet the CTBT requirements for xenon monitoring. The proposed schedule calls for a three phase test which should be completed by the end of the year 2000. The first phase will allow development and completion of the Russian and Swedish systems. Phase two will involve installation and simultaneous testing of all four systems at the Institute for Atmospheric Research in Freiburg, Germany. It is expected that this phase will take one or two months and be completed in early 2000. The third phase will be a test of xenon systems at future International Monitoring System (IMS) sites at locations yet to be chosen. The purpose of this phase is to demonstrate long-term, unattended operation to gain experience on measurements without highly skilled technical operators in attendance.

The ARSA system developed by PNNL is ready now to participate in these tests and we are confident that the ARSA system will satisfy all the requirements for xenon monitoring for CTBT verification.

REFERENCES

- [1] L. R. Mason, J. D. Bohner, D. L. Williams, Int. Conf. Meth. and Appl. of Radioanal. Chem., Kailua-Kona, HI, April 6-11, 1997, J. Radioanal. Nucl. Chem. **235**, 65 (1998).
- [2] T. W. Bowyer, R. W. Perkins, K. H. Abel, W. K. Hensley, C. W. Hubbard, A. D. McKinnon, M. E. Panisko, P. L. Reeder, R. C. Thompson, and R. A. Warner, Xenon Radionuclides, Atmospheric: Monitoring, Encyclopedia of Environmental Analysis and Remediation, Robert A. Myers, Ed., John Wiley and Sons, 1998, pp. 5299-5314.
- [3] T. W. Bowyer, K. H. Abel, C. W. Hubbard, M. E. Panisko, P. L. Reeder, R. C. Thompson, and R. A. Warner, J. Radioanal. Nucl. Chem. **240**, 109 (1999).
- [4] E. Browne and R. B. Firestone, "Table of Radioactive Isotopes", John Wiley and Sons, Inc., New York, 1986.
- [5] ENDF/B-VI, National Nuclear Data Center, Brookhaven, NY.
- [6] T. W. Bowyer, K. H. Abel, C. W. Hubbard, A. D. McKinnon, M. E. Panisko, R. W. Perkins, P. L. Reeder, R. C. Thompson, and R. A. Warner, Int. Conf. Meth. and Appl. of Radioanal. Chem., Kailua-Kona, HI, April 6-11, 1997, J. Radioanal. Nucl. Chem. **235**, 77 (1998).
- [7] P. L. Reeder, T. W. Bowyer, and R. W. Perkins, Int. Conf. Meth. and Appl. of Radioanal. Chem., Kailua-Kona, HI, April 6-11, 1997, J. Radioanal. Nucl. Chem. **235**, 89 (1998).
- [8] P. L. Reeder and T. W. Bowyer, Nucl. Instrum. Meth. Phys. Res. A **408**, 573 (1998).
- [9] P. L. Reeder and T. W. Bowyer, Nucl. Instrum. Meth. Phys. Res. A **408**, 582 (1998).
- [10] P. L. Reeder, T. W. Bowyer, and K. H. Abel, "Analysis of Beta-Gated Gamma Spectra for the PNNL ARSA and Estimate of Minimum Detectable Activities for ($^{131\text{m}}\text{Xe}+^{133\text{m}}\text{Xe}$), ^{133}Xe , and ^{135}Xe ", PNNL-11784-Rev. 1, March 1998.